www.czasopisma.pan.pl PAN www.journals.pan.pl

ARCHIVES of FOUNDRY ENGINEERING

ISSN (2299-2944)
Volume 19
Issue 2/2019

79 – 84

10.24425/afe.2019.127120

14/2

Published quarterly as the organ of the Foundry Commission of the Polish Academy of Sciences

Dispersion of Al-Si Alloy Structure by Intensive Pulsed Electron Beam

S. Konovalov [a, b, *], V. Gromov [c], D. Zaguliyaev [c], Y. Ivanov [d], A. Semin [c], J. Rubannikova [c]

[a] Wenzhou University, China
[b] Samara National Research University, Russia
[c] Siberian State Industrial University, Russia
[d] Institute of High Current Electronics SB RAS, Russia
* Corresponding author. E-mail address: ksv@ssau.ru

Received 27.03.2019; accepted in revised form 06.05.2019

Abstract

By the method of modern physical material science (optic microscopy scanning and transmission electron microscopy) the analysis of structural phase states, the morphology of the second phase inclusions and defect substructure of Al-Si alloy (silumin) of hypoeutectic composition, subjected to electron beam processing was done with the following parameters: energy density 25-35 J/cm^2, beam length 150 μs, pulse number – 3, pulse repetition rate – 0.3 Hz, pressure of residual gas (argon) 0.02 Pa. The surface irradiation results in the melting of the surface layer, the dissolution of boundary inclusions, the stricture formation of high speed cellular crystallization of submicron sizes, the repeated precipitation of the second phase nanodimentional particles. With the increased distance from the irradiation surface the layer containing the second phase inclusions of quasi-equilibrium shape along with the crystallization cells was revealed. It is indicative of the processes of Al-Si alloy structure globalization on electron beam processing.

Keywords: Silumin structure, Electron beam processing, Crystallization cells, Dispersion

1. Introduction

The foundry alloys of Al-Si system (silumins) are characterized by the high yielding, average plasticity, good strength and hardness [1]. The principal specifications of the manufactured products are determined by the method of casting and the presence of thermal treatment. So, for the hypoeutectic alloy $AlSi_{10}Mg_2Ni$ the rupture strength is in the range of 180-270 MPa, the elongation per unit length is 1.4-1.5 % and the hardness is 70-85 HV. Silumins are widely used in the automobile industry for manufacturing of various parts working at different loads, normal and increased temperatures (for example, for the casting of internal combustion engine, frames for different purposes, parts of devices etc.). The main disadvantage of silumins is the high brittleness caused by the presence of big silicon and intermetallide inclusions as well as the pores. Whose quantity increases, as a rule, with the increase in silicon concentration in the alloy [2-5].

At present, methods have been developed to control the formation of the structure and properties of aluminum alloys through the use of various physical methods for treating melts in the processes of melting and crystallization. For these purposes, tested methods such as temperature-speed and temperature-time processing [6-9], the effects of magnetic and electric fields [10-12], ultrasonic and vibration processing [13-15], and several others.

One of the method of formation of nanodimentional structural phase states and alloys, metalloceramic and ceramic materials is pulsed regime of super high speed heating and cooling of surface layer. Nowadays, the most promising from the positions of nanostructuring is the application of highly intense pulsed ion and electron heat beams of submillisecond duration, making it

possible to heat with control of the surface layers of ten micrometers thickness in the pulsed regime practically without changing of structural phase state of the bulk of the material [16 - 24]. In comparison with the widely distributed laser, flame and ion types of effect the electron beam technology has the more flexible possibilities of control and regulation of supplied energy and it differs by high locality of effect and high efficiency. It is outlined in the studies of researches [25 - 34] that the processing of eutectic and hypereutectic silumin and another metals by electron beams results in the essential modification of properties in the material surface under the influence of dynamic stress fields generated when heating, melting and cooling. This modification is associated with the considerable refining of structure, the improvement of wear and corrosion resistance, and the increase in hardness. For both the researchers and technological purposes the low energy (5-20 keV) pulsed (50-200 μs) electron beams may be considered the promising ones, they ensure the energy density (up to 100 J/cm^2) in the wide range on the surface of the irradiated material and super high rates of heating (up to 10^6 K/s) to the preset temperature followed by surface layer cooling at the expense of heath removal in the bulk of material at the rate of 10^4-10^9 K/s at the limiting gradients of temperature (up to 10^7-10^8 K/m) [25 - 34].

The physical meaning of effect of nanodimentional structural phase states on the strength and plastic properties of the surface consists in the redistribution of elastic energy both at the expense of the interaction of elastic fields of structural elements of different scale level and the decrease in the scale level of plastic deformation localization. It results in the more uniform distribution of elastic stresses in the surface layer under the external mechanical and/ or temperature effect. As result the energy required for the nucleation of critical stress concentrators increases considerably and the essential decrease in the rate of microcracks growth takes phase, the strength and plasticity of not only the surface layer but also the sample as a whore increases [23 - 34].

The purpose of the paper is the analysis of structural phase state evolution of aluminium foundry hypoeutectic alloy subjected to the irradiation in vacuum by the intense pulsed electron beam.

2. Material and methods

Aluminium foundry hypoeutectic Al-Si alloy (silumin) (11.1 Si, 0.58 Mg, 2.19 Cu, 0.92 Ni, 0.25 Fe, 0.029 Mn, 0.047 Ti, 0.005 Cr, balance Al (weight %)) [34] was used as a tests material. The samples were in the form of 20×20×10 mm plates. At least 10 samples were used.

The modification of surface layer structure was done by irradiating the samples of the alloy in vacuum by the intense pulsed electron beam at the unit SOLO (Institute of High Current Electronics SB RAS) [23, 34]. The irradiation parameters were following: the energy of accelerated electrons 17 keV, the energy density of electron beam 25, 30, 35 J/cm^2, pulse length of electron beam 150 μs, number of pulses 3, pulse repetition rate 0.3 s^{-1}, pressure of residual gas (argon) in the working chamber of the unit 2×10^{-2} Pa. The used parameters contributed to the best increase (more than 2 times) in the fatigue life of silumin [23]. The structure of the samples was tested by method of optic microscopy (metallographic microvisor μVizo-MET-221), scanning (Philips SEM-515 with microanalyser EDAX ECON IV) and transmission (JEM-2100F, JEOL) electron microscopy. The elemental composition of silumin was analyzed by micro X-ray spectrum analysis methods.

The foil preparation included the electrolytic etching of plates (thickness 150-200 nm), which were cut out of modified samples parallel to the treated surface using an electrospark erosion method.

3. Results and discussion

The Al-Si alloy in the cast state is characterized by the presence of a large quantity of the second phase inclusions of different elemental composition, various shapes and sizes (Figure 1). The other adverse factor of the cast alloy structure is the presence of micropores (Fig. 1, micropores are show by the arrows).

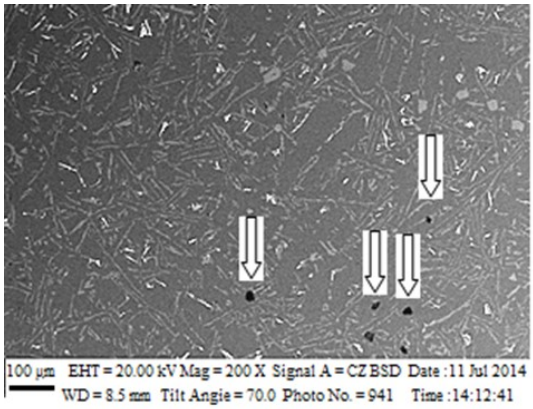

Fig. 1. Structure of alloy AlSi10Mg2Ni in the cast state. Micropores are shown by the arrows

The surface irradiation of silumin samples by the intense pulsed electron beam with the parameters indicated above results in the in the cardinal transformation of the structural phase state of the material surface layer. In 50-100 μm thick layer whose sizes increase with the increase in the energy density of electron beam the structure of cellular crystallization characteristic of the quickly hardened material (Figure 2) is formed. The second phase inclusions of the foundry origin in the surface layer are not observed.

The elemental composition of the second phase inclusions is analyzed, as a rule, by the methods of metallography using specially selected reagents or by the methods of micro X-ray spectrum analysis using scanning electron microscopy [35, 36]. These methods enable one to carry out express analysis for the distribution of the alloying and impurity elements in the material after casting and their redistribution on subsequent treatment (thermal and thermomechanical). In spite of high promptitude the indicated methods possess a comparatively low accuracy and insufficient locality of determination of the inclusion elemental composition. In the present paper the main research method of silumin elemental composition in the cast state and after

irradiation by the intense pulsed electron beam is the method of micro X-ray spectroscopic analysis of thin foils and it practically eliminated the possibility of imposing of several inclusions located in the volume of the analyzed foil of the sample.

Figures 3 and 4 show the example of micro X-ray spectroscopic analysis of the lamellar type inclusion being present in the alloy.

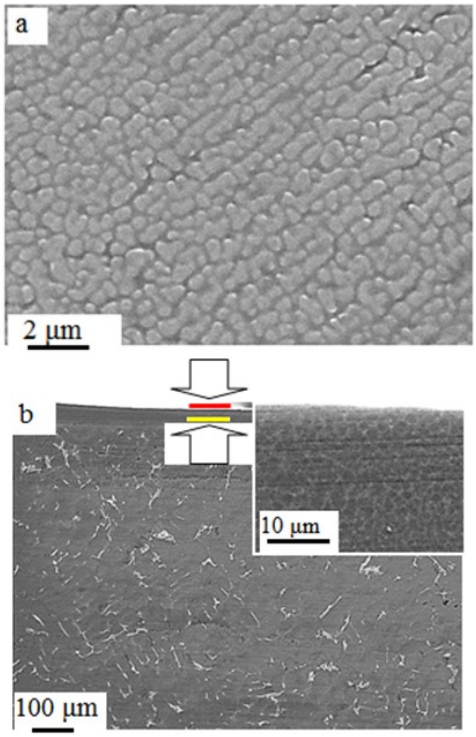

Fig. 2. Structure of Al-Si alloy irradiated by the intense pulsed electron beam (35 J/cm^2, 150 µs, 3 pulses); (a) structure of irradiation surface; (b) structure of the transverse metallographic section (the layer of high speed crystallization is indicated by the lines and arrows)

As it has been mentioned above (Figure 2), the silumin irradiation by the intense pulsed electron beam is accompanied by the melting of thin surface layer, the dissolution of the second phase inclusions and formation of the cellular crystallization structure at the stage of cooling. The characteristic image of the stricture of silumin surface layer irradiated by the electron beam is shown in Figure 5. The average size of cells increases within 0.3 µm to 0.6 µm with the increase in the energy density of electron beam (25-35 J/cm^2) for the invariable other parameters of irradiation. The cells are separated by the thin interlayers of the second phase, the transverse sizes of the interlayers are less than 100 nm (Figure 5, b).

The results of the sampling quantitative analysis of the elemental composition of the second phase inclusions being present in silumin in the cast state are given in Table 1. When analyzing the results given in Table 1 the multi-elemental composition of the majority of the inclusions can be noted.

When analyzing the results shown in Table 2 it can be noted that the irradiation of silumin by intense pulsed electron beam in the regime of the surface layer melting results, firstly, in the homogenization of the elemental composition of the surface layer; secondly, the decrease in the concentration of silicon atoms in the surface layer, enhancing with the increase in energy density of electron beam. Table 2 shows the elemental composition of different portions of silumin surface layer irradiated by the electron beam.

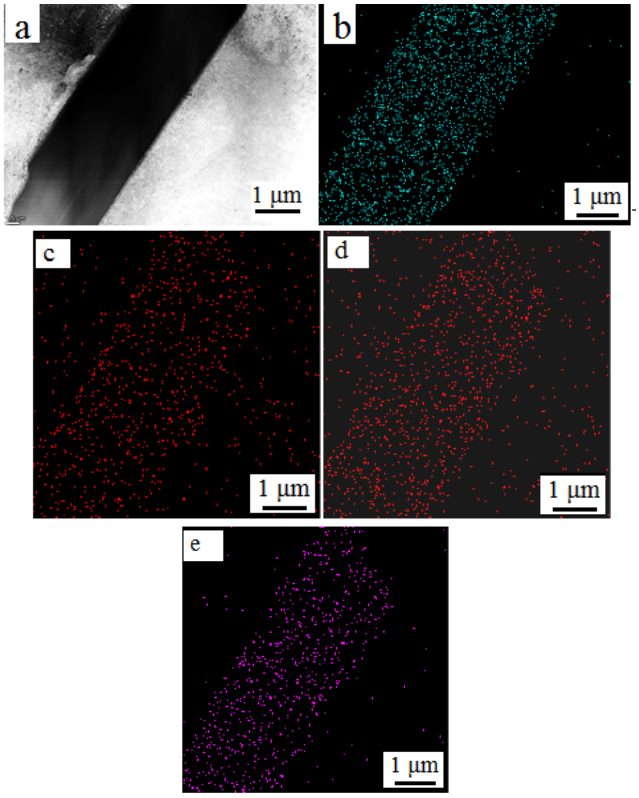

Fig. 3. Electron microscope image of Al-Si alloy on the cast state (a); b – d give the image of the same portion of the foil obtained in the characteristic X-ray radiation of Ni (b), Si (c), Cu (d) and Fe (e) atoms

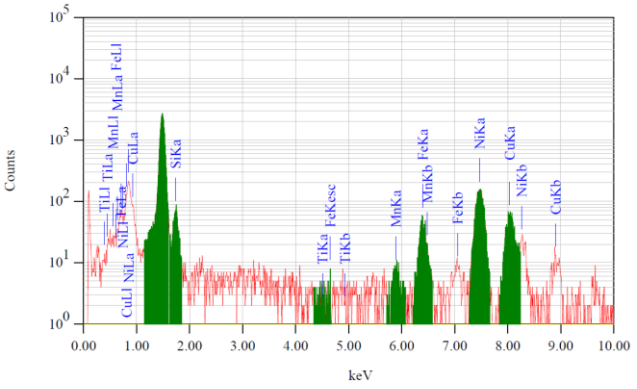

Fig. 4. Energy spectra obtained from the foil portion show in Figure 3, a

Table 1.
Results of micro X-ray spectroscopic analysis of the second phase inclusions of the cast silumin

Element	Concentration, at. %									
	Number of portion of micro X-ray spectroscopic analysis									
	1	2	3	4	5	6	7	8	9	10
Mg	0.07	0.0	2.36	0.0	0.0	0.0	0.0	0.0	0.0	0.0
Al	79.6	84.79	64.69	87.47	73.73	80.77	79.99	98.32	82.89	82.67
Si	18.48	12.3	31.38	1.12	26.08	8.05	13.1	0.0	0.0	16.24
Ti	0.1	0.69	0.02	0.03	0.09	0.14	0.46	0.08	0.02	0.05
Mn	0.04	0.06	0.04	0.15	0.08	0.24	0.04	0.02	0.07	0.0
Fe	0.25	0.47	0.38	1.76	0.0	1.71	1.48	0.05	0.1	0.02
Ni	0.0	0.13	0.18	6.51	0.01	6.22	3.02	0.04	3.15	0.01
Cu	1.47	1.56	0.95	2.95	1.0	2.86	1.91	1.5	13.77	1.01

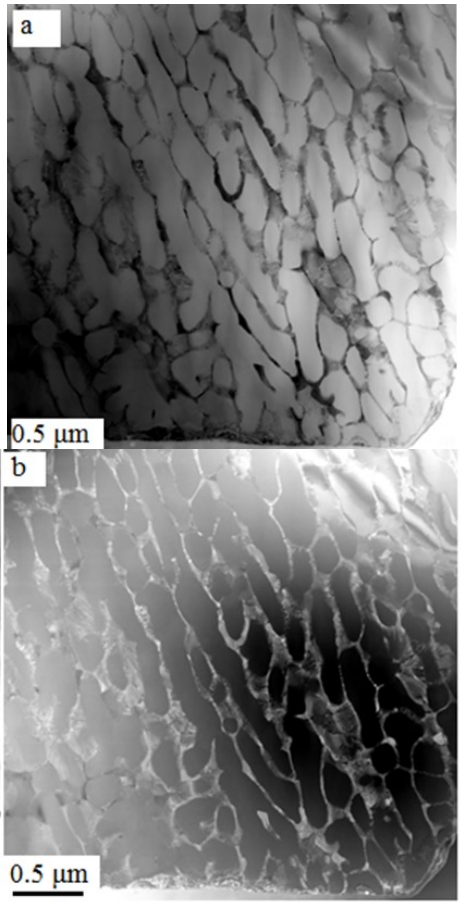

Fig. 5. Electron microscope image of silumin surface layer structure obtained in vacuum by intense pulsed electron beam (35 J/cm^2, 150 µs, 3 pulsed). The transmission electron microscopy in the regime of scanning; a – light field image; b – dark field image

Table 2.
Elemental composition of different regions of cellular substructure of silumin surface layer irradiated by intense electron beam

Element	Concentration, at. %								
	Number of portion of micro X-ray spectroscopic analysis								
	*1 / 25	2 / 25	3 / 25	4 / 25	5 / 30	6 / 30	7 / 30	8 / 35	9 / 35
Mg	0.32	0.81	0.44	1.28	0.0	0.14	0.0	0.0	0.0
Al	90.14	89.41	86.83	89.82	92.14	90.97	91.77	91.1	92.83
Si	7.15	6.88	10.36	6.13	5.86	6.25	6.17	3.68	4.69
Ti	0.11	0.13	0.11	0.08	0.04	0.05	0.01	0.13	0.25
Mn	0.02	0.01	0.02	0.02	0.0	0.01	0.0	0.04	0.02
Fe	0.11	0.24	0.12	0.14	0.14	0.07	0.12	0.59	0.1
Ni	0.2	0.6	0.28	0.36	0.37	0.61	0.41	2.02	0.45
Cu	1.94	1.9	1.83	2.17	1.45	1.9	1.53	2.44	1.67

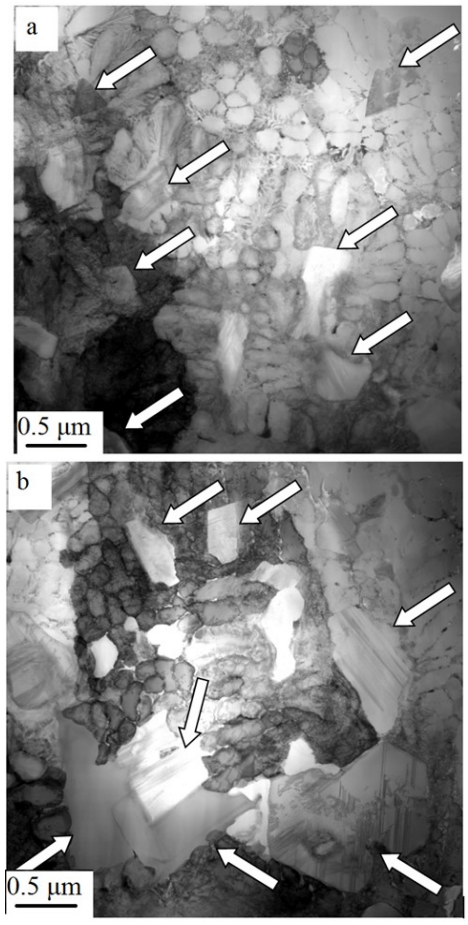

Fig. 6. Structure of silumin irradiated by intense pulsed electron beam (35 J/cm^2, 150 µs, 3 pulses); a - the layer at 70 µm depth; b – the layer at 90 µm depth. The inclusions cast origin are shown by the arrows

The irradiation of silumin by intense pulsed electron beam is accompanied by the formation of gradient structure – the structure

of cellular crystallization transforms, when moving away from the surface of processing, to the structure of the mixed type where partly dissolved inclusions of the foundry origin (Figure 6) are present along with the cells. When analyzing the structure of the given transmission layer, the absence of the lamellar shape inclusions in it can be noted. In the majority of cases the inclusions have a quasi-equilibrium shape (Figure 6, a). This statement is true for both the silicon particles and the particles of intermetallics. It should be noted that the globularization of silicon and intermetallics particles should essentially increase the plastic properties not only of the modified layer but also the material as a whole.

4. Conclusion

The evolution analysis of the elemental composition and the defect structure, the morphology of the second phase inclusions in aluminium foundry hypoeutectic alloy subjected to the irradiation by intense pulsed electron beam in vacuum was done. It was stated that the irradiation of silumin by the electron beam in the regime of surface layer melting was accompanied by the dissolution of the foundry inclusions, the homogenization of the elemental composition, the formation of the structure of high speed cellular crystallization, the repeated precipitation of nanodimentional particles of the second phase. It is show that the modified layer has the gradient structure. The surface layer with submicro-nanodimentional structure of cellular crystallization goes into the layer containing the second phase inclusions of quasi – equilibrium shape along with the cells of crystallization. It gives evidence of the processes of materials globularization on the irradiation of silumin by electron beam.

Acknowledgements

The work was supported by the state task of the Ministry of education and science of the Russian Federation, project № 3.1283.2017/4.6).

Reference

[1] Szymczak, T., Gumienny, G. & Pacyniak, T. (2016). Effect of Cr and W on the Crystallization Process, the Microstructure and Properties of Hypoeutectic Silumin to Pressure Die Casting. *Archives of Foundry Engineering*. 16(3), 109-114. DOI: 10.1515/afe-2016-0060.

[2] Majernik, J., Gaspar, S., Gryc, K. & Socha, L. (2018). Changes in eutectic silumin structure depending on gate geometry and its effect on mechanical properties of casting. *Manufacturing Technology*. 18(3), 439-443. DOI: 10.21062/ujep/118.2018/a/1213-2489/MT/18/3/439.

[3] Szymczak, T., Gumienny, G. & Pacyniak, T. (2015). Effect of Vanadium and Molybdenum on the Crystallization, Microstructure and Properties of Hypoeutectic Silumin. *Archives of Foundry Engineering*. 15(4), 81-86. DOI: 10.1515/afe-2015-0084.

[4] Szymczak, T., Gumienny, G., Pacyniak, T. & Walas, K. (2015). Effect of tungsten and molybdenum on the crystallization, microstructure and properties of silumin 226. *Archives of Foundry Engineering*. 15(3), 61-66. DOI: 10.1515/afe-2015-0061.

[5] Pasko, J., Gaspar, S. & Ruzbarsky, J. (2014). Die casting defects of castings from silumin. *Applied Mechanics and Materials*. 510, 91-96. DOI: 10.4028/www.scientific.net /AMM.510.91.

[6] Deev, V.B., Prusov, E.S. & Kutsenko A.I. (2018). Theoretical and experimental evaluation of the effectiveness of aluminum melt treatment by physical methods. *Metallurgia Italiana*. 110(2), 16-24.

[7] Deev, V.B., Ponomareva, K.V. & Yudin, A.S. (2015). Investigation into the density of polystyrene foam models when implementing the resource-saving fabrication technology of thin-wall aluminum sheet. *Russian Journal of Non-Ferrous Metals*. 56(3), 283-286. DOI: 10.3103/ S1067821215030049.

[8] Li, Q.L., Xia, T.D., Lan, Y.F. & Li, P.F. (2014). Effects of melt superheat treatment on microstructure and wear behaviours of hypereutectic Al–20Si alloy. *Materials Science and Technology (United Kingdom)*. 30 (7), 835-841. DOI: 10.1179/1743284713Y.0000000415.

[9] Yang, W., Yang, X. & Ji, S. (2015). Melt superheating on the microstructure and mechanical properties of diecast Al–Mg–Si–Mn alloy. *Metals and Materials International*. 21(2), 382-390. DOI: 10.1007/s12540-015-4215-2

[10] Zhang, Y., Rabiger, D., Willers, B. & Eckert, S. (2017). The effect of pulsed electrical currents on the formation of macrosegregation in solidifying Al–Si hypoeutectic phases. *International Journal of Cast Metals Research*. 30, 13-19. DOI: 10.1080/13640461.2016.1174455.

[11] Krymsky, V. & Shaburova, N. (2018). Applying of Pulsed Electromagnetic Processing of Melts in Laboratory and Industrial Conditions. *Materials.* 11(6), 954. DOI: 10.3390/ma11060954.

[12] Zheng, T., Zhou, B., Zhong, Y., Wang, J., Shuai, S., Ren, Z., Debray, F. & Beaugnon, E. (2019). Solute trapping in Al-Cu alloys caused by a 29 Tesla super high static magnetic field. *Scientific Reports*. 9(1), 266. DOI: 10.1038/s41598-018-36303-5.

[13] Vorozhtsov, S., Kudryashova, O., Promakhov, V., Dammer, V. & Vorozhtsov, A. (2016). Theoretical and experimental investigations of the process of vibration treatment of liquid metals containing nanoparticles. *JOM*. 68(12), 3094-3100. DOI: 10.1007/s11837-016-2147-z.

[14] Zhang, Y., Svynarenko, K. & Li, T. (2016). Effect of ultrasonic treatment on formation of iron-containing intermetallic compounds in Al–Si alloys. *China Foundry*. 13(5), 316-321. DOI: 10.1007/s41230-016-5066-2.

[15] Eskin, D.G. (2017). Ultrasonic processing of molten and solidifying aluminium alloys: overview and outlook. *Materials Science and Technology (United Kingdom)*. 33(6), 636-645. DOI: 10.1080/02670836.2016.1162415.

[16] Panin, S.V., Maruschak, P.O., Vlasov, I.V., Sergeev, V.P., Ovechkin, B.B. & Neifeld, V.V. (2016). Impact toughness of

12Cr1MoV steel. Part 2 - Influence of high intensity ion beam irradiation on energy and deformation parameters and mechanisms of fracture. *Theoretical and Applied Fracture Mechanics*. 83, 82-92. DOI: 10.1016/j.tafmec.2015.12.009.

[17] Panin, S.V., Vlasov, I.V., Sergeev, V.P., Ovechkin, B.B., Marushchak, P.O., Ramasubbu, S., Lyubutin, P.S. & Titkov, V.V. (2015). Fatigue life enhancement by irradiation of 12Cr1MoV steel with a Zr+ ion beam. Mesoscale deformation and fracture. *Physical Mesomechanics*. 18 (3), 261-272. DOI: 10.1134/S1029959915030108.

[18] Ramazanov, K.N., Vafin, R.K. & Khusainov, Yu, G. (2014). Ion nitriding of tool steel kh12 in glow discharge in cross electric and magnetic fields. *Metal Science and Heat Treatment*. 56(1-2), 50-52. DOI: 10.1007/s11041-014-9701-5.

[19] Budilov, V.V., Ramazanov, K.N. & Vafin, R.K. (2011). Ion nitriding of tool steels with application of magnetic field. *Metal Science and Heat Treatment*. 53 (7-8), 347-349. DOI: 10.1007/s11041-011-9395-x.

[20] Ghyngazov, S.A., Vasil'ev, I.P., Surzhikov, A.P., Frangulyan, T.S. & Chernyavskii, A.V. (2015). Ion processing of zirconium ceramics by high-power pulsed beams. *Technical Physics*. 60(1), 128-132. DOI: 10.1134/S1063784215010120.

[21] Fomin, A.A. & Gusev, V.G. (2013) Vibrational displacement of a spindle with static disequilibrium of the cutting tool. *Russian Engineering Research*. 33(7), 412-415. DOI: 10.3103/S1068798X1307006X.

[22] Surzhikov, A.P., Frangulyan, T.S., Ghyngazov, S.A. & Vasil'ev, I.P. (2014). The effect of a low-energy high-current pulsed electron beam on surface layers of porous zirconium ceramics. *Technical Physics Letters*. 40 (9), 762-765. DOI: 10.1134/S1063785014090144.

[23] Ivanov, Y.F., Alsaraeva, K.V., Gromov, V.E., Popova & N.A., Konovalov, S.V. (2015). Fatigue life of silumin treated with a high-intensity pulsed electron beam. *Journal of Surface Investigation*. 9(5), 1056-1059. DOI: 10.1134/S1027451015050328.

[24] Zagulyaev, D., Konovalov, S., Gromov, V., Glezer, A., Ivanov, Y. & Sundeev, R. (2018). Structure and properties changes of Al-Si alloy treated by pulsed electron beam. *Materials Letters*. 229, 377-380. DOI: 10.1016/j.matlet.2018.07.064.

[25] An, J., Shen, X.X., Lu, Y., Liu, Y.B., Li, R.G., Chen, C.M. & Zhang, M.J. (2006). Influence of high current pulsed electron beam treatment on the tribological properties of Al-Si-Pb alloy. *Surface and Coatings Technology*. 200(18-19), 5590-5597. DOI: 10.1016/j.surfcoat.2005.07.106.

[26] Hao, S., Yao, S., Guan, J., Wu, A., Zhong, P. & Dong, C. (2001). Surface treatment of aluminum by high current pulsed electron beam. *Current Applied Physics*. 1(2-3), 203-208. DOI: 10.1016/S1567-1739(01)00017-7.

[27] Yan, P., Grosdidier, T., Zhang, X. & Zou, J. (2018). Formation of large grains by epitaxial and abnormal growth at the surface of pulsed electron beam treated metallic samples. *Materials and Design*. 159, 1-10. DOI: 10.1016/j.matdes.2018.08.033.

[28] Zhang, C., Lv, P., Cai, J., Zhang, Y., Xia, H. & Guan, Q. (2017). Enhanced corrosion property of W-Al coatings fabricated on aluminum using surface alloying under high-current pulsed electron beam. *Journal of Alloys and Compounds*. 723, 258-265. DOI: 10.1016/j.jallcom.2017.06.189.

[29] Park, K., Park, J. & Kwon, H. (2017). Fabrication and characterization of Al-SUS316L composite materials manufactured by the spark plasma sintering process. *Materials Science and Engineering A*. 691, 8-15. DOI: 10.1016/j.msea.2017.03.029.

[30] Gao, B., Hao, Y., Tu, G., Li, S., Yu, F., Zuo, L. & Hu, L. (2013). Surface modification of Mg 67 -Zn 30 -Y 3 quasicrystal alloy by high current pulsed electron beam. *Surface and Coatings Technology*. 229, 42-45. DOI: 10.1016/j.surfcoat.2012.06.026.

[31] Gao, B., Xu, N. & Xing, P. (2019). Shock wave induced nanocrystallization during the high current pulsed electron beam process and its effect on mechanical properties. *Materials Letters*. 237, 180-184. DOI: 10.1016/j.matlet.2018.11.054

[32] Lyu, J., Gao, B., Hu, L., Lu, S. & Tu, G. (2016). Microstructure analysis of HPb59-1 brass induced by high current pulsed electron beam. *High Temperature Materials and Processes*. 35(7), 715-721. DOI: 10.1515/htmp-2015-0030.

[33] Gao, B., Hao, S., Zou, J., Wu, W., Tu, G. & Dong, C. (2007). Effect of high current pulsed electron beam treatment on surface microstructure and wear and corrosion resistance of an AZ91HP magnesium alloy. *Surface and Coatings Technology*. 201(14), 6297-6303. DOI: 10.1016/j.surfcoat.2006.11.036.

[34] Gao, B., Hao, S., Zou, J., Grosdidier, T., Jiang, L., Zhou, J. & Dong, C. (2005). High current pulsed electron beam treatment of AZ31 Mg alloy. *Journal of Vacuum Science and Technology A: Vacuum, Surfaces and Films*. 23(6), 1548-1553. DOI: 10.1116/1.2049299.

[35] Zolotorevsky, V.S., Belov, N.A. & Glazoff, M.V. (2007). *Casting Aluminium Alloys.* Oxford: Elsevier.

[36] Goldstein, J.I., Newbury, D.E., Michael, J.R., Ritchie, N.W.M., Scott, J.H.J. & Joy, D.C. (2017) *Scanning electron microscopy and x-ray microanalysis.* New York: Springer.